The crystal structure of gurmarin, a sweet taste-suppressing protein: Identification of the amino acid residues essential for inhibition

Maud Sigoillot, Anne Brockoff, Fabrice Neiers, Nicolas Poirier, Christine Belloir, Pierre Legrand, Christophe Charron, Pierre Roblin, Wolfgang Meyerhof, Loïc Briand

Journal : CHEMSE

Article Doi : 10.1093/chemse/bjy054

OXFORD
UNIVERSITY PRESS

Article Title : The Crystal Structure of Gurmarin, a Sweet Taste–Suppressing Protein: Identification of the Amino Acid Residues Essential for Inhibition

INSTRUCTIONS

1. **Author groups:** Please check that all names have been spelled correctly and appear in the correct order. Please also check that all initials are present. Please check that the author surnames (family name) have been correctly identified by a pink background. If this is incorrect, please identify the full surname of the relevant authors. Occasionally, the distinction between surnames and forenames can be ambiguous, and this is to ensure that the authors' full surnames and forenames are tagged correctly, for accurate indexing online. Please also check all author affiliations.
2. **Figures:** If applicable figures have been placed as close as possible to their first citation. Please check that they are complete and that the correct figure legend is present. Figures in the proof are low resolution versions that will be replaced with high resolution versions when the journal is printed.
3. **Colour reproduction:** These figures are currently intended to appear online in colour and black and white in print. Please check the black and white versions (these may be available at the end of the paper) and contact us if you have any concerns. Please re-word the legend/text to avoid using reference to colour. Alternatively, please let us know if you wish to pay for print colour reproduction or to have both versions in black and white. Please note that there is a £350/$600 charge for each figure reproduced in colour in print.
4. **Missing elements:** Please check that the text is complete and that all figures, tables and their legends are included.
5. **Special characters:** Please check that special characters, equations, dosages and units, if applicable, have been reproduced accurately.
6. **URLs:** Please check that all web addresses cited in the text, footnotes and reference list are up-to-date, and please provide a 'last accessed' date for each URL.
7. **Funding:** Please provide a Funding statement, detailing any funding received. Remember that any funding used while completing this work should be highlighted in a separate Funding section. Please ensure that you use the full official name of the funding body, and if your paper has received funding from any institution, such as NIH, please inform us of the grant number to go into the funding section. We use the institution names to tag NIH-funded articles so they are deposited at PMC. If we already have this information, we will have tagged it and it will appear as coloured text in the funding paragraph. Please check the information is correct. [red text to be used for suppliers who are tagging the funding]
8. Authors receive a 50% discount on colour figure reproduction if the author is a member of ECRO, AChemS or JASTS.

MAKING CORRECTIONS TO YOUR PROOF

These instructions show you how to mark changes or add notes to your proofs using Adobe Acrobat Professional versions 7 and onwards, or Adobe Reader DC. To check what version you are using go to **Help** then **About**. The latest version of Adobe Reader is available for free from get.adobe.com/reader.

DO NOT OVERWRITE TEXT, USE COMMENTING TOOLS ONLY.

DISPLAYING THE TOOLBARS

Adobe Reader DC

In Adobe Reader DC, the Comment toolbar can be found by clicking 'Comment' in the menu on the right-hand side of the page (shown below).

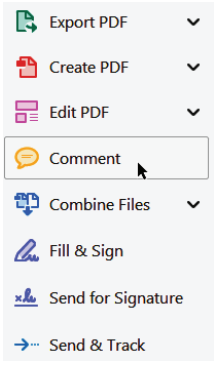

The toolbar shown below will then display along the top.

Acrobat Professional 7, 8, and 9

In Adobe Professional, the Comment toolbar can be found by clicking 'Comment(s)' in the top toolbar, and then clicking 'Show Comment & Markup Toolbar' (shown below).

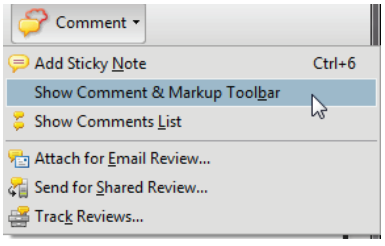

The toolbar shown below will then be displayed along the top.

USING TEXT EDITS AND COMMENTS IN ACROBAT

This is the quickest, simplest and easiest method both to make corrections, and for your corrections to be transferred and checked.

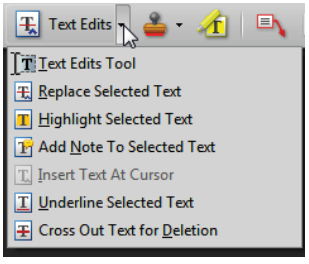

1. Click **Text Edits**
2. Select the text to be annotated or place your cursor at the insertion point and start typing.
3. Click the **Text Edits** drop down arrow and select the required action.

You can also right click on selected text for a range of commenting options, or add sticky notes.

SAVING COMMENTS

In order to save your comments and notes, you need to save the file (**File, Save**) when you close the document.

USING COMMENTING TOOLS IN ADOBE READER

All commenting tools are displayed in the toolbar.
To edit your document, use the highlighter, sticky notes, and the variety of insert/replace text options.

POP-UP NOTES

In both Reader and Acrobat, when you insert or edit text a pop-up box will appear. In **Acrobat** it looks like this:

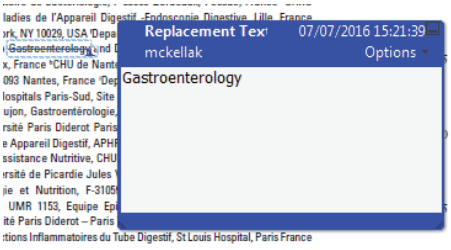

In **Reader** it looks like this, and will appear in the right-hand pane:

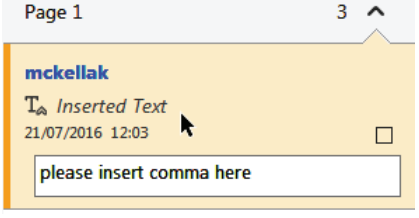

AUTHOR QUERY FORM

Journal : CHEMSE

Article Doi : 10.1093/chemse/bjy054

Article Title : The Crystal Structure of Gurmarin, a Sweet Taste–Suppressing Protein: Identification of the Amino Acid Residues Essential for Inhibition

First Author : Maud Sigoillot

Corr. Author : Loïc Briand

AUTHOR QUERIES - TO BE ANSWERED BY THE CORRESPONDING AUTHOR

The following queries have arisen during the typesetting of your manuscript. Please click on each query number and respond by indicating the change required within the text of the article. If no change is needed please add a note saying "No change."

AQ1	Please check the edits in the article title.
AQ2	Resolution for all the supplied figures are found to be low than usually printed. Please provide high resolution images for better processing.
AQ3	Please check that all names have been spelled correctly and appear in the correct order. Please also check that all initials are present. Please check that the author surnames (family name) have been correctly identified by a pink background. If this is incorrect, please identify the full surname of the relevant authors. Occasionally, the distinction between surnames and forenames can be ambiguous, and this is to ensure that the authors' full surnames and forenames are tagged correctly, for accurate indexing online. Please also check all author affiliations.
AQ4	Please provide the department name (if any) in affiliations 1 and 5.
AQ5	Please review the typeset tables carefully against copies of the originals to verify accuracy of editing and typesetting.
AQ6	Please define DMEM.
AQ7	Figures have been placed as close as possible to their first citation. Please check that they have no missing sections and that the correct figure legend is present.
AQ8	The reference "Sigoillot et al. 2002a" is not included in the reference list. Please include the citation in the list with full publication detail.
AQ9	Please check the edits in the "Funding" section.
AQ10	Please provide the abbreviated journal title in the reference "Sheldrick 2008".

Chemical Senses, 2018, Vol XX, 1–9
doi:10.1093/chemse/bjy054
Original Article
Advance Access publication 18 August 2018

Original Article

The Crystal Structure of Gurmarin, a Sweet Taste–Suppressing Protein: Identification of the Amino Acid Residues Essential for Inhibition

Maud Sigoillot[1], Anne Brockhoff[2], Fabrice Neiers[1], Nicolas Poirier[1], Christine Belloir[1], Pierre Legrand[3], Christophe Charron[4], Pierre Roblin[3], Wolfgang Meyerhof[2,5] and Loïc Briand[1]

[1]INRA, CNRS, Centre des Sciences du Goût et de l'Alimentation, Université de Bourgogne-Franche Comté, 21000 Dijon, France, [2]Department of Molecular Genetics, German Institute of Human Nutrition, Potsdam-Rehbruecke, Arthur-Scheunert-Allee 114–116, 14558 Nuthetal, Germany, [3]SOLEIL Synchrotron, L'Orme de Merisiers, Saint-Aubin, 91192 Gif-sur-Yvette, France, [4]Ingénierie Moléculaire et Physiopathologie Articulaire, Centre National de la Recherche Scientifique Unité Mixte de Recherche 7365, Université de Lorraine, Biopôle de l'Université de Lorraine, 54505 Vandoeuvre-les-Nancy Cedex, France and [5]Present address: Center for Integrative Physiology and Molecular Medicine (CIPMM), Saarland University, Kirrbergerstrasse, Bldg. 48, 66421 Homburg, Germany

Correspondence to be sent to: Loïc Briand, INRA, CNRS, Centre des Sciences du Goût et de l'Alimentation, Université de Bourgogne-Franche Comté, Dijon 21000, France. e-mail: loic.briand@inra.fr

Editorial Decision 3 August 2018.

Abstract

Gurmarin is a highly specific sweet taste–suppressing protein in rodents that is isolated from the Indian plant *Gymnema sylvestre*. Gurmarin consists of 35 amino acid residues containing 3 intramolecular disulfide bridges that form a cystine knot. Here, we report the crystal structure of gurmarin at a 1.45 Å resolution and compare it with previously reported nuclear magnetic resonance solution structures. The atomic structure at this resolution allowed us to identify a very flexible region consisting of hydrophobic residues. Some of these amino acid residues had been identified as a putative binding site for the rat sweet taste receptor in a previous study. By combining alanine-scanning mutagenesis of the gurmarin molecule and a functional cell-based receptor assay, we confirmed that some single point mutations in these positions drastically affect sweet taste receptor inhibition by gurmarin.

Key words: *Gymnema sylvestre*, G protein-coupled receptor, inhibitor, knottin, sweet taste, taste receptor

Introduction

Gurmarin is a polypeptide isolated from the leaves of the Indian plant *Gymnema sylvestre* (Imoto et al. 1991a). Gurmarin selectively inhibits the sweet taste in rats and mice but only has a weak effect in humans (Imoto et al. 1991a,b; Miyasaka and Imoto 1995; Ninomiya and Imoto 1995). A peculiar feature of gurmarin is its long-lasting inhibition. Several hours (>2–3 h) have been shown to be necessary for complete recovery of the sweet tasting function in rats (Imoto et al. 1991a; Murata et al. 2003). Gurmarin is composed of 35 amino acid residues and 3 disulfide bonds. Three-dimensional structures of natural and synthetic gurmarin have been solved (Arai et al. 1995; Fletcher et al. 1999) using ^{1}H nuclear magnetic resonance (NMR) at pH 2.9 and 298 K (protein data bank [PDB] entries 1GUR and 1C4E, respectively). Gurmarin belongs to the structural family of cysteine-knot miniproteins, called knottins, which have been identified in various organisms, including fungi, plants, arthropods, and vertebrates. Members of this family have diverse functions, including antimicrobial activity, protease

inhibition, and toxicity (Pallaghy et al. 1994). Members of this family share structural motifs, including a disulfide bond framework and a core of 3 antiparallel beta sheets with one or more loops of variable length that interact with various targets (Pallaghy et al. 1994; Postic et al. 2018). These structural features confer high stability, rigidity, and remarkable proteolysis resistance to knottins, which makes these proteins promising scaffolds for the development of therapeutic and diagnostic agents (Kimura et al. 2009; Moore et al. 2013).

The sweet taste receptor is a heterodimer formed by the assembly of 2 distinct subunits: T1r2 and T1r3 (Nelson et al. 2001; Li et al. 2002). The T1r2 and T1r3 subunits are members of the small family of class C G protein-coupled receptors (GPCRs), which includes the metabotropic glutamate receptors, calcium-sensing receptor, and γ-aminobutyric acid receptor B. T1r2 and T1r3-like class C GPCRs share a common architecture, including a large N-terminal domain (NTD) connected to the heptahelical transmembrane domain (TM) via a short cysteine-rich domain (CRD). The NTD of T1r2 contains the primary binding sites for sweet compounds (Behrens and Meyerhof 2011). However, at least 2 other binding sites have been identified in the sweet taste receptor, allowing it to bind a large panel of compounds (Belloir et al. 2017). One binding site is located in the NTD of T1r3 (Nie et al. 2005; Maitrepierre et al. 2012), and the other binding site is located in the TM of the same subunit. Although the molecular mechanism of sweetness inhibition is not clearly understood, it has been shown that gurmarin acts via the rodent heterodimeric T1r2/T1r3 sweet taste receptor (Margolskee et al. 2007; Sigoillot et al. 2012a; Kojima et al. 2014; Medina et al. 2014). Exposure of mouse T1r2/T1r3 heterologously expressed in human embryonic kidney (HEK) 293 cells to gurmarin caused complete inhibition of intracellular calcium mobilization in response to sucralose, saccharin, and acesulfame K (Margolskee et al. 2007; Sigoillot et al. 2012a). Furthermore, gurmarin blocked the sucralose-induced release of GLP-1 and GIP from murine enteroendocrine GLUTag cells, presumably via inhibition of the endogenously expressed sweet taste receptor (Margolskee et al. 2007). More recently, gurmarin has been used to highlight the involvement of T1r2/T1r3 in the regulation of energy homeostasis in murine neurons (Kohno et al. 2016). Interestingly, gurmarin has also been used to block amino acid sensing via mice umami T1r1/T1r3 in the gut (Vancleef et al. 2015). We have proposed 2 models of inhibition in which gurmarin binds to the N-terminal domain of the T1r3 subunit (Sigoillot et al. 2012b). In the first model, gurmarin binds within the 2 lobes composing the NTD of T1R3, preventing closure of the T1r2 or T1r1 NTDs, thus inactivating both umami and sweet taste receptors. Alternatively, gurmarin may interact with the hydrophobic dimerization interface between subunits, preventing the closed conformations of both NTDs, which have been shown to be critical for class C GPCR activation (Pin et al. 2003; Kniazeff et al. 2011).

We previously reported that recombinant gurmarin expressed in *Pichia pastoris* is functional and leads to complete blockage of saccharin-induced fluorescence responses in rat T1r2/T1r3-expressing cells, with an IC_{50} value of 7.1 nM but has no effect on the human T1r2/T1r3 receptor (Sigoillot et al. 2012a). Here, we report the crystal structure of recombinant gurmarin determined at a high resolution of 1.45 Å, which allowed us to identify several flexible amino acid residues located in the putative binding interface with the T1r2/T1r3 sweet taste receptor. To further characterize the binding mode of gurmarin, we generated independent alanine substitutions of the residues in the putative binding site. We then measured the ability of gurmarin mutants to suppress saccharin-induced responses from functionally expressed rat T1r2/T1r3 (rT1r2/rT1r3) in a cell-based assay.

Materials and Methods

Production and purification of gurmarin mutants

Wild-type and mutant gurmarin proteins were produced using the yeast *P. pastoris*. The secreted proteins were purified as previously reported (Sigoillot et al. 2012a). The vector pPIC9-gurm was used as the template for site-directed mutagenesis using a polymerase chain reaction-based protocol (QuikChange Multi Site-Directed Mutagenesis kit, Stratagene). The sequences of the generated mutants were verified by automated DNA sequencing (Beckman coulters genomics). *P. pastoris* GS115 cells were transformed by electroporation, and the best protein-producing transformants (His^+ Mut^S) were identified by SDS-PAGE. Single isolated colonies were used to inoculate 50 mL of buffered minimal glycerol-complex medium in a 500 mL baffled flask, which was then incubated at 29 °C while shaking at 300 rpm for 16 h. Twenty milliliters of this preculture were then used to inoculate 1 L of buffered glycerol-complex medium, which was divided between 4 3-L baffled flasks. The flasks were then incubated at 29 °C while shaking at 300 rpm for 2 days. The cells were pelleted at 3000 *g* for 20 min at room temperature, and the supernatant was discarded. *Pichia* cells were resuspended in 1 L of buffered minimal methanol medium at pH 6.0, which was divided between 4 sterile 3 L baffled flasks and incubated at 29 °C while shaking at 300 rpm for 4 days. Methanol was added every 24 h. Wild-type and mutant gurmarin proteins were purified by cation-exchange chromatography and reversed phase chromatography as previously described (Sigoillot et al. 2012a).

Far-UV circular dichroism analysis

Far-UV circular dichroism (CD) spectra were recorded using a JASCO J-815 spectropolarimeter equipped with a Peltier temperature control set at 25 °C. A protein concentration of 300 µM in 20 mM sodium acetate buffer, pH 4.0, was used for measurements of the wild-type and mutant gurmarin proteins. Using a 0.01 cm path length quartz cell, the spectra were recorded with a scan speed of 50 nm/min between 190 and 260 nm. The spectra were averaged over 15 scans and corrected by subtraction of the spectra acquired for buffer alone. The CD measurements are presented as molar ellipticity $deg.cm^2.dmol^{-1}$ using the Jasco Spectra Analysis software.

Crystallization and data collection

Purified wild-type gurmarin was concentrated to 15 mg/mL using a Vivacon 2 ultrafiltration device (Sartorius Stedim Biotech GmbH). The protein concentration was measured with a NanoDropND-1000 spectrophotometer (NanoDrop Technologies, Inc.). Crystals of recombinant gurmarin, consisting of Q1E-gur, were obtained by the hanging-drop vapor-diffusion method. The hanging drop was formed by mixing an equal volume of protein solution with 20 mM sodium citrate pH 4.0 and equilibration against a reservoir containing 100 mM MES pH 6.8, 5 mM $MgCl_2$, 5 mM $CaCl_2$, 50 mM $CdCl_2$, 50 mM $NiCl_2$, and 12% (w/v) PEG 3350 at 293 K. Diffraction data of gurmarin crystals cocrystallized with nickel was collected at 100 K at the SOLEIL synchrotron on the PROXIMA-1 beamline up to a resolution of 1.45 Å. To maximize the maximum high resolution (due to experimental limitations on the detector to crystal minimum distance), diffraction was recorded away from the peak absorption edge of nickel at a

AQ5 **Table 1.** Data collection and refinement statistics

Data collection	Gurmarin (Ni-SAD)
PDB	5OLL
Source	SOLEIL PROXIMA-1
Wavelength (Å)	1.0332
Space group	*R3*
Cell parameters (Å)	$a = b = 53.6$
	$c = 38.1$
Cell Angles (°)	$\alpha = \beta = 90$
	$\gamma = 120$
Resolution limits[a] (Å)	30–1.45 (1.49–1.45)
Rmerge[a] (%)	5.1 (80.0)
CC1/2 (%)	99.8 (70.0)
Unique reflections[a]	7211 (523)
Mean((I)/sd(I))[a]	18.1 (1.9)
Completeness[a] (%)	99.9 (99.9)
Multiplicity[a]	5.5 (5.5)
Refinement	
Resolution[a] (Å)	12 -1.45 (1.62–1.45)
Number of reflections[a]	7238 (1952)
Number of test set reflections	362 (103)
Number of protein / water / ligand atoms	293/37/3 Ni2+
R_{work}/R_{free} [a]	0.190/0.191 (0.232/0.262)
R.M.S.D bonds (Å)/angles (°)	0.010/1.13
B-wilson/B-average (Å^2)	24.8/35.0
Ramachandran: preferred/allowed/outliers (%)	93.9/6.1/0

[a]Numbers in brackets refer to the highest resolution bin.

wavelength of 1.0332 Å. Diffraction data (Table 1) were processed with XDS package (Kabsch 2010).

Structure solution and refinement

Despite 2 nickel sites located at special positions, the usable phases were calculated by single-wavelength anomalous diffraction due to a third nickel site and solvent flattening, which allowed us to overcome phase ambiguity. The SHELX C/D/E program package (Sheldrick 2008) was used to find the nickel positions and calculate the initial phases leading to interpretable maps. Subsequently, several cycles of model building using COOT (Emsley et al. 2010) combined with refinement using BUSTER-TNT-2.10 (Bricogne et al. 2017) were conducted. Finally, structure validation was performed with MOLPROBITY (Chen et al. 2010).

3D-structure alignment

~~The gurmarin structural homologues were screened using the PDBe Fold program (Gutmanas et al. 2014), which is available online (http://www.ebi.ac.uk/msd-srv/ssm/cgi-bin/ssmserver). The 9 most relevant homologues were selected on the basis of the alignment length and the root-mean-square deviation (RMSD).~~ The crystal structure was aligned with the 2 NMR structures (PDB entry 1GUR and 1C4E) using SUPERPOSE in the CCP4 suite (Krissinel 2012).

Functional assay of recombinant gurmarin proteins

The ability of gurmarin mutants to suppress sweetener-induced responses from the rat sweet taste receptor heterodimer was assessed using PEAKrapid cells (modified HEK293 cells, American Type Culture Collection) that stably express $mG\alpha_{15}$ and HEK293T cells stably expressing the chimeric G protein Gα16gust44. To optimize coexpression of both receptor subunits, we generated a pcDNA3-based (Invitrogen) expression vector containing the coding sequences of both rT1r2 and rT1r3 according to the cloning strategy of Ariyasu et al. 2003. Cells were maintained under standard culture conditions (37 °C, 5% CO_2) in ~~DMEM,~~ high glucose (Invitrogen) supplied with AQ6 10% FCS-To (v/v), 100 U/mL penicillin, 100 mg/mL streptomycin, and 2 mM glutamine. Prior to the experiment, cells were seeded onto 96-well plates coated with poly-D-lysine (10 µg/mL) and transfected using Lipofectamine2000 (Invitrogen). Cells transfected with empty vector (mock) served as a negative control. After 48 h, cells were loaded with the fluorescent calcium indicator dye Fluo-4 AM (2 µM in DMEM low glucose GlutaMAX with 2.5 mM probenicid) and incubated for 1 h at 37 °C. Excess dye was washed off twice using a bath solution (130 mM NaCl, 10 mM Na-Hepes pH 7.4, 10 mM pyruvate, 5 mM KCl, 2 mM $CaCl_2$). Between washing steps, cells were incubated for 40 min at room temperature to allow complete de-esterification of the dye. Test compounds were dissolved in the bath solution. As reported previously, cells were preincubated with recombinant gurmarin proteins for 10 min (Sigoillot et al. 2012a). After a thorough washing, cells were subsequently challenged with saccharin. Fluorescence signals upon automated application of gurmarin proteins and saccharin were recorded at λ 510 nm after excitation at λ 488 nm using a FLIPR Tetra (Molecular Devices). For consecutive measurements, saccharin was washed off and the cells were maintained at room temperature in the dark. Prior to the measurement, 60 min after gurmarin preincubation, the same cells were rewashed and challenged with saccharin for a second time. After the last stimulation, the cell vitality and number were controlled by bath application of the β-adrenoreceptor agonist isoproterenol. Inhibition responses were calculated as described previously (Sigoillot et al. 2012a). Data were collected from at least 3 independent experiments carried out in duplicate.

Results

Crystal structure of gurmarin

To solve the crystal structure of gurmarin, we purified the recombinant protein secreted by the yeast *P. pastoris* as previously reported (Sigoillot et al. 2012a). Crystallization of gurmarin was achieved using the hanging drop vapor-diffusion method at pH 6.8 with PEG 3350 as the precipitant in the presence of various cations. Numerous crystals of gurmarin were obtained after 2 weeks. The crystals of gurmarin obtained under this condition belonged to space group ~~*H3*~~ *R3*, with unit-cell parameters $a = b = 53.6$ Å, $c = 38.1$ Å. The crystal structure was solved at a high resolution of 1.45 Å. As shown in Figure 1A, with the exception of the loops' positioning, the global backbone fold of crystallized gurmarin is similar to those of the NMR structures of natural gurmarin purified from the plant *G. sylvestre* (Arai et al. 1995); (PDB accession code 1GUR). The gurmarin secondary structure consists of an antiparallel β-sheet stabilized with disulfide bonds. Six cysteine residues form 3 intramolecular disulfide bonds, Cys3-Cys18, Cys10-Cys23, and Cys18-Cys33 (Figure 2A), with a characteristic knotted arrangement, as previously reported (Arai et al. 1995; Fletcher et al. 1999). The backbone RMSD difference of the alpha carbon (residues 2–35) between the first crystal structure gurmarin and the 2 reported NMR structures were 1.63 and 1.81 Å for the 1GUR and 1C4E PDB files, respectively (Arai et al. 1995; Fletcher et al. 1999). These differences can be explained by positioning differences in the loops and the N- and C-termini parts (Figure 1A). It should be noted that these types of differences with NMR solved structures are usual, and the RMSD of the backbone (residues 3 ± 34) between the 2 NMR structures is 1.61 Å.

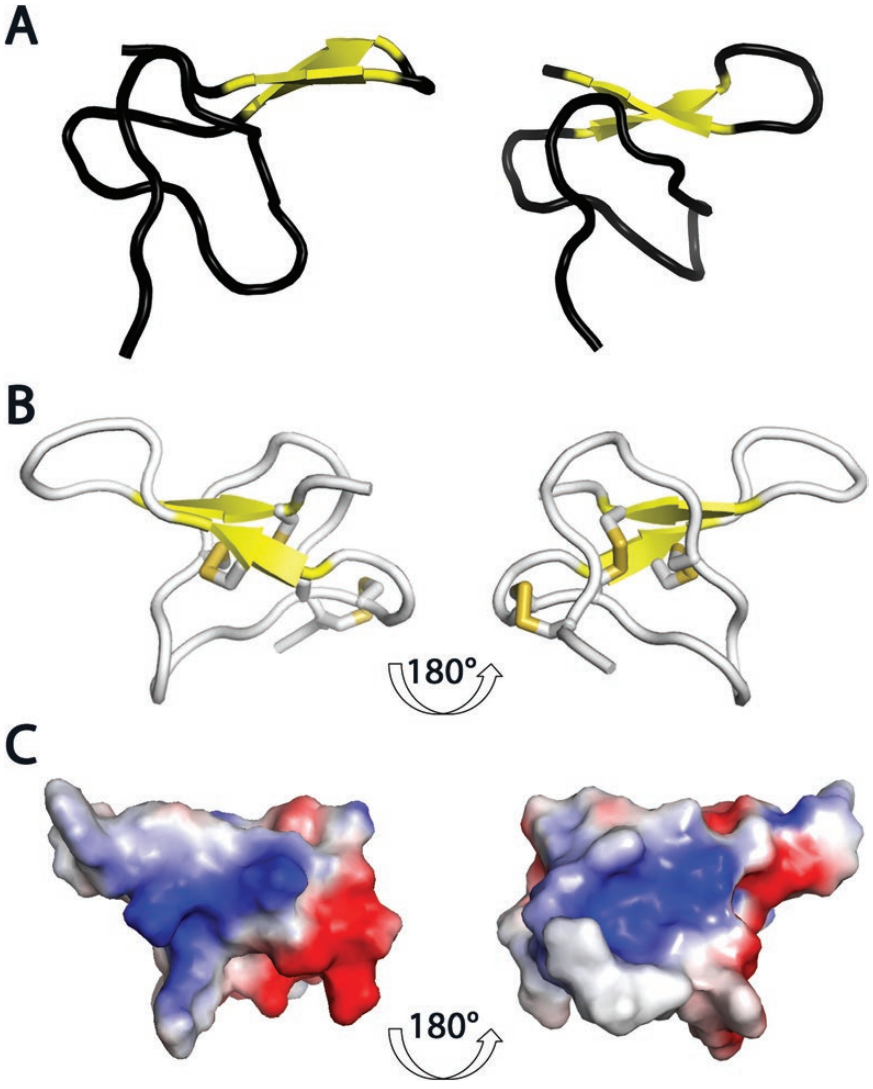

Figure 1. Structural views of gurmarin. (A) Comparison of the NMR (left) and X-ray (right) gurmarin structures. (B) The 2 views are related by a 180° rotation of the X-ray gurmarin structure. The beta-strand is represented in yellow, and the 3 disulfide bridges are represented as sticks. (C) Distribution of hydrophobic and hydrophilic residues at the gurmarin surface. The views are related by a 180° rotation. The negatively charged amino acid residues are in red, the positively charged residues are in blue and the neutral residues are in white.

These differences also explain our failure to use the NMR structures as models for molecular replacement to solve the gurmarin X-ray structure. The 2 NMR structures present differences in different area compared to the crystal structure (Figure 2C). Some regions as the loop containing the tryptophan residues are different in the 3 structures (Figure 2C). Also, the differences in the side chain positioning and more particularly in this area are important (Figure 2B). Although the X-ray structure was solved at a high resolution, we found that the side chains of the tryptophan residues W28 and W29 were poorly defined, revealing the high degree of mobility of these amino acid residues (Figure 3B). This observation is also supported by a higher Boltzmann value (B-value), which is represented in red in Figure 3C, for these positions. The B-value indicates the mobility of the atoms in the structure: the higher the B-value, the higher the mobility. Interestingly, the side chains of residues Y14 and W28 were solved in 2 distinct conformations, which also supports the flexibility of these residues (Figure 3B). This observation is in good agreement with our previous NMR study (Sigoillot et al. 2012a). Indeed, using ^{15}N HSQC experiments conducted at 318 K and 298 K, we previously showed that the intensity of several crosspeaks (between amino acid residues Y14, L15, and D16) was dramatically decreased at the lowest temperature tested suggesting a dynamic behavior of these residues. The crystal structure and the previous NMR data confirm a dynamic behavior for the Y13–D16 amino acid stretch, particularly for the 2 tryptophan residues W28 and W29 (Figure 3A). Also, the crystal packing reveals that this area is free of intermolecular interaction leading to a particular positioning of these residues.

Distribution of important residues for the inhibition properties of gurmarin

The inhibitory properties of gurmarin have been previously linked to a group of amino acids (L9, I11, P12, Y13, Y14, W28, and W29) whose side chains form an outwardly directed hydrophobic cluster at the surface of the molecule (Ota et al. 1998). To investigate whether the flexible residues identified in the crystal structure of gurmarin are involved in the site of interaction with the sweet T1r2/T1r3 taste receptor, we performed alanine substitution using site-directed mutagenesis of the amino acid residues L9, I11, Y13, Y14,

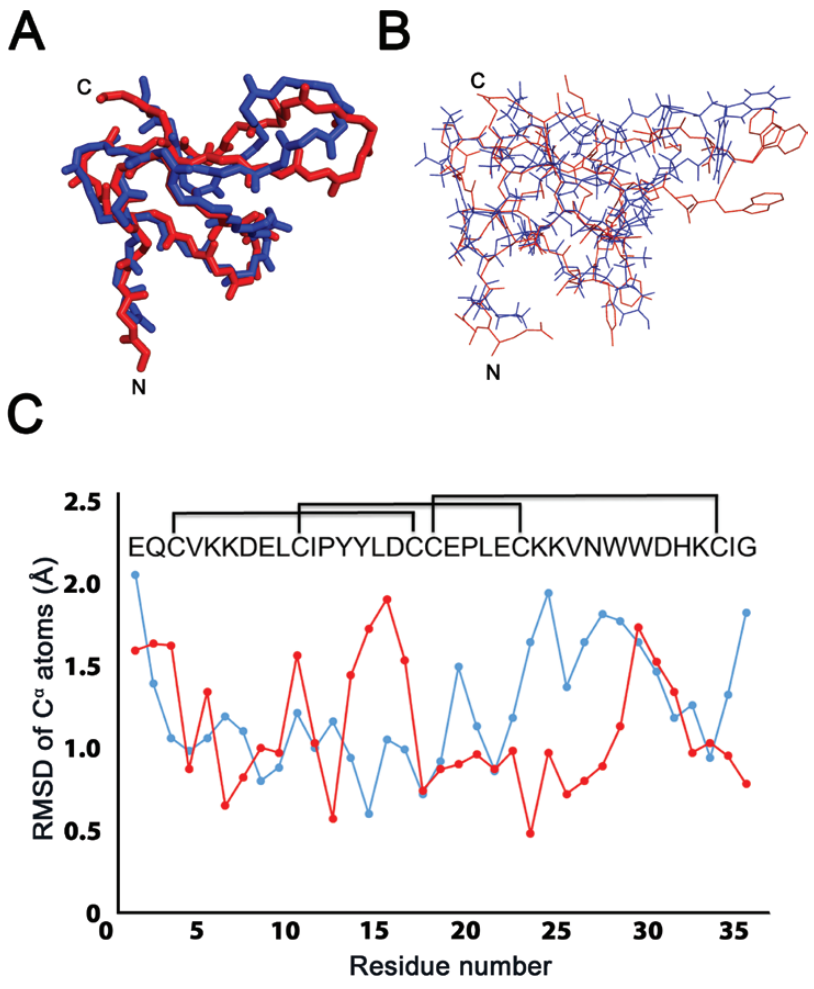

Figure 2. Comparison of the crystal structure and solution structures of gurmarin. (A) The main chain of the gurmarin X-ray structure is superposed to the main chain of the gurmarin NMR solution structure (PDB entry 1C4E). (B) The main and side chains of the gurmarin X-ray structure are superposed to the main and side chains of the gurmarin NMR solution structure (PDB entry 1C4E). (C) The crystal structure is aligned with the 2 NMR structures (PDB entry 1GUR and 1C4E) using SUPERPOSE in the CCP4 suite. For each residues number of the NMR structures (red plots for 1GUR and blue plots for 1C4E), the RMSD of the C^{α} atom indicating the comparison with the crystal structure is plotted. The gurmarin sequence is also indicated with the disulfide bridges.

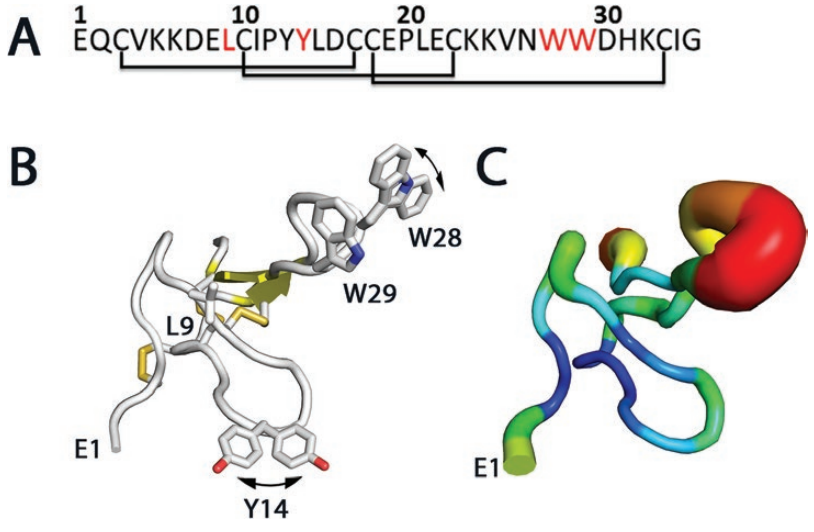

Figure 3. Positions of mutated amino acids in the gurmarin protein. (A) Amino acid sequence of gurmarin, with the disulfide-bonding pattern indicated by lines below the sequence. The amino acids mutated in this study are indicated in red. (B) Cartoon view of gurmarin. The residues mutated in the study are shown in stick mode. (C) B-factor analysis along the backbone chain of gurmarin in cartoon mode. B-factor analysis along the backbone chain of the gurmarin was performed using the Pymol program. Residues showing the lowest and highest mobility are represented with cold and hot colours, respectively.

W28, and W29. The mutated gurmarin proteins were secreted by the yeast *P. pastoris* and purified as described for wild-type gurmarin (Figure 4). Unfortunately, due to severely impaired yeast secretion levels, the gurmarin mutants I11A and Y13A could not be investigated. This observation suggests that these 2 amino acid residues have an impact on protein secretion, refolding or protein stability. To examine whether alanine substitution affected the protein folding of secreted and purified mutants, we used CD spectroscopy, a sensitive technique for determining the protein conformation and estimate protein secondary structure. Gurmarin is a small compact polypeptide stabilized by 3 disulfide bonds with 35 amino acid residues containing 2 tyrosine, 2 tryptophan residues, and many of these side chains are in close proximity (Figure 3A). Such aromatic chromophore stackings are important since they may contribute heavily to the far-UV CD spectrum (Sreerama *et al.* 1999). As previously reported (Sigoillot et al. ~~2002a~~), wild-type gurmarin has an unusual far-UV CD spectrum (Figure 5). It has 2 negative bands centered at 220 and 227 nm, respectively. The sharp negative band at 220 nm is consistent with the presence of β-structures, whereas the negative is characteristic from the contribution of aromatic clusters. We found that the CD spectrum of wild-type gurmarin is quite different of those of each of the mutants, Y14A mutant exhibiting the largest difference (Figure 5). These changes in spectral shape of gurmarin mutants may be attributed to slight alterations in the environments of the aromatic side chains. Because the substitutions have been made outside the disulfide bonds network, we can expect that these amino acid substitutions have a low impact on the 3-dimensional structure of gurmarin.

Suppressive effect of gurmarin mutants on the functionally expressed rat sweet taste receptor

We previously demonstrated that recombinant gurmarin, produced by the methylotropic yeast *P. pastoris*, is capable of selectively suppressing sweetener-induced responses from cells that heterologously express the rat sweet taste receptor (Sigoillot et al. 2012a). Cells expressing the human sweet taste receptor heterodimer were insensitive to recombinant gurmarin. To determine the functional effect of individual mutations of the gurmarin hydrophobic cluster residues,

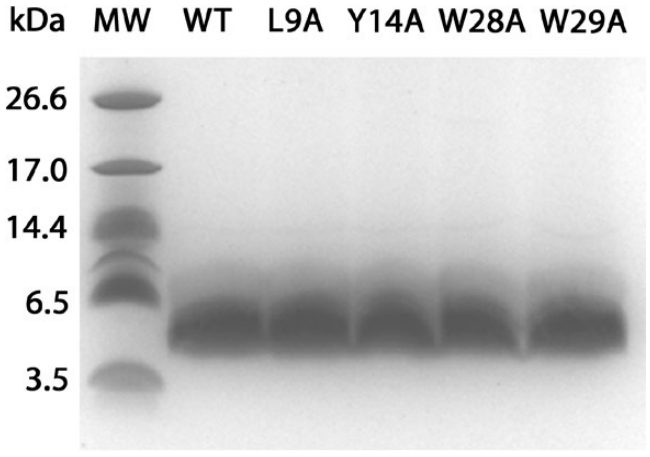

Figure 4. SDS-PAGE analysis of the purified wild-type and mutated gurmarin. Lane 1, molecular weight standard marker (Polypeptide SDS-PAGE standards, Bio-Rad). Lane 2–6, purified wild-type and gurmarin mutants. Proteins were visualized by Coomassie Brilliant Blue G-250 staining.

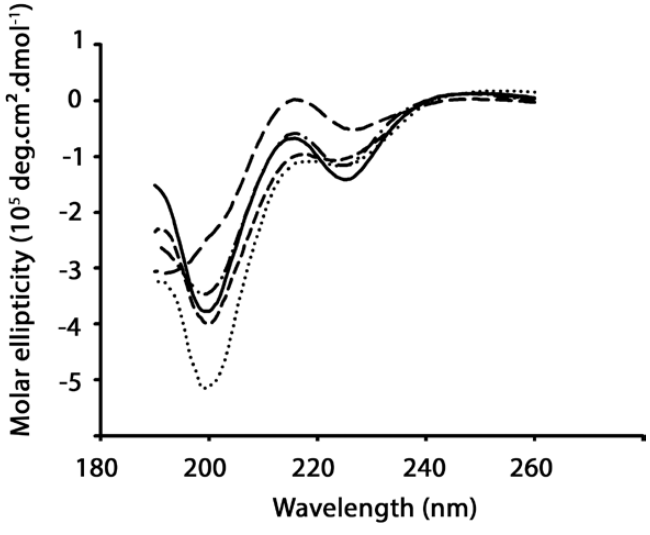

Figure 5. Secondary structure analysis by circular dichroism. Far-UV CD spectra of wild-type gurmarin (solid curve), gurmarin L9A (dot and dash curve), gurmarin Y14A (long dash curve), gurmarin W28A (short dash curve), and gurmarin W29A (dot curve). Spectra were recorded at 25 °C with a 0.01-cm path cell length and a 300 μM protein concentration in a 20 mM sodium acetate buffer, pH 4.0.

we tested their inhibitory capacity using a functional cell-based assay, as previously reported (Sigoillot et al. 2012a). Preincubation of HEK cells expressing rat T1r2/T1r3 with recombinant gurmarin mutants at their maximum applicable concentration (30 µg/mL) did not induce calcium fluorescence signals (Figure 6A, top row), indicating that the introduced mutations did not elicit artificial reactions from the cellular background. More importantly, the mutations did not reverse the antagonistic properties of gurmarin. After washing off the gurmarin mutants, cells were subsequently challenged with the sweet taste receptor agonist saccharin (7 mM; ~EC_{90}). Preincubation with recombinant wild-type gurmarin completely blocked cellular responses to saccharin (Figure 6A, second row). By contrast, introduction of alanine substitutions at hydrophobic cluster positions rendered gurmarin less effective. To different extents, residual responses to saccharin revealed that none of the gurmarin mutants was capable of fully inhibiting rT1r2/rT1r3 activity within the tested concentration range. Remarkably, mutation of W29 to alanine completely abolished the sweet-suppressing properties of gurmarin within the applicable compound concentration of 30 µg/mL. Upon pretreatment with the gurmarin W29A mutant, the cellular responses to saccharin were unaffected, which was apparent by comparing the saccharin fluorescence signals to those of untreated cells (Figure 6A, sixth vs. first column).

To study the impact of individual mutations of gurmarin hydrophobic cluster residues in detail, we recorded inhibition responses over a range of concentrations and calculated the values of the half-maximal effective concentrations (IC_{50}). Subsequent to the preincubation with wild-type gurmarin, cellular responses to saccharin (7 mM, ~EC_{90}) were dose-dependently inhibited with an IC_{50} of ~0.03 µg/mL and entirely blocked at 0.3 µg/mL (Figure 6B). Introducing alanine

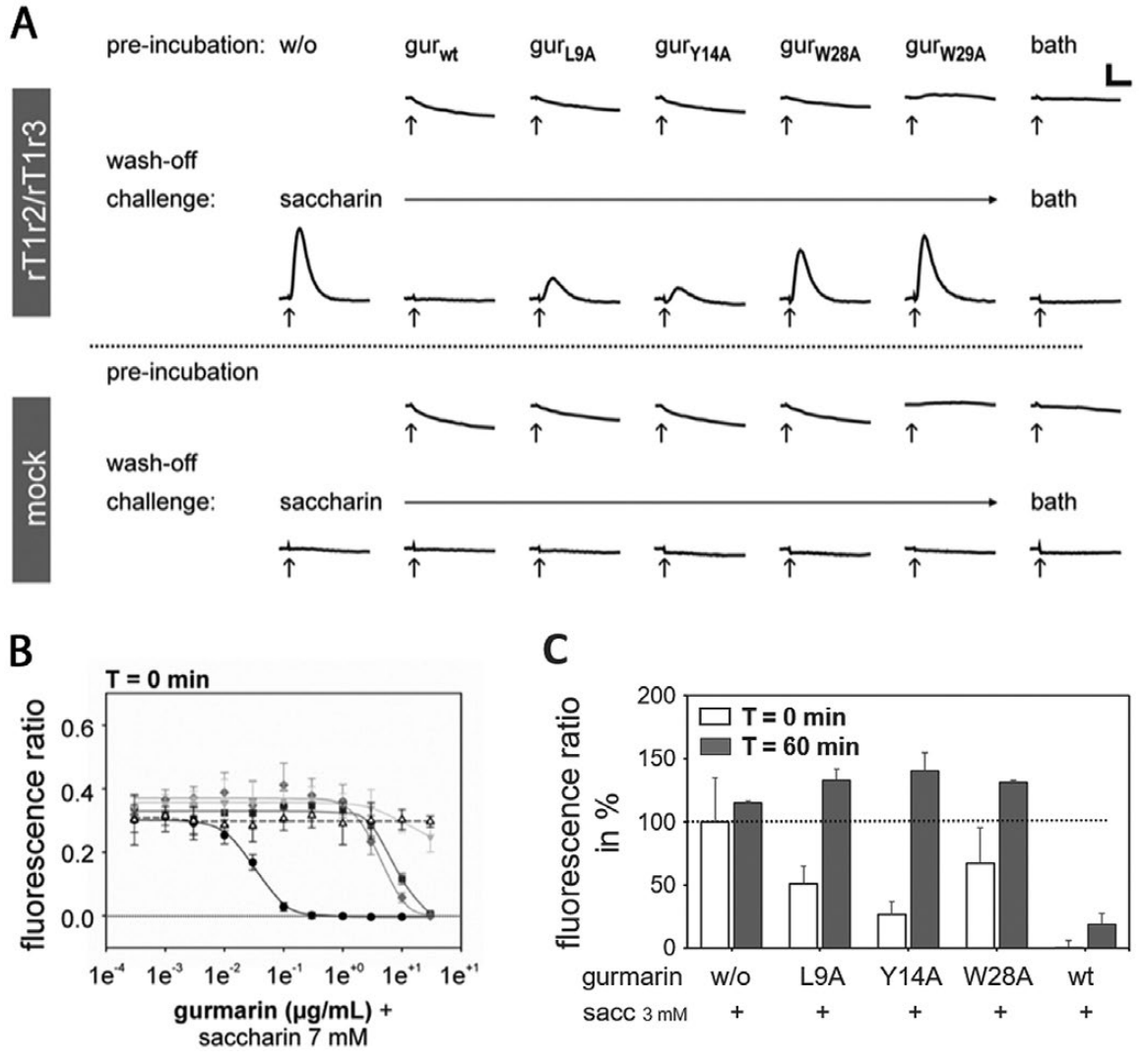

Figure 6. Hydrophobic cluster residues are crucial for the sweet suppressive effect of gurmarin on rT1R2/rT1R3-expressing cells. (A) Representative calcium fluorescence traces of PEAKrapid mGα15 cells transfected with the rT1r2/rT1r3 expression construct (upper rows) and empty vector (lower rows). Cells were preincubated (↑) with gurmarin variants (10 µg/mL) for 10 min. After a thorough washing, cells were challenged with the sweetener saccharin (7 mM). Scale: y, 100 counts; x, 50 s. (B) Inhibition responses from PEAKrapid mGα15 cells expressing rT1r2/rT1r3 after preincubation with increasing concentrations of gurmarin variants. Black circles, wild-type gurmarin. Dark gray squares, gurmarin L9A. Medium gray diamonds, gurmarin Y14A. Light gray triangles, gurmarin W28A. White triangles, gurmarin W29A. Reference line, fluorescence ratio 0.0. (C) Time course fluorescence signal ratios of rT1r2/rT1r3-expressing HEK293T Gα16gust44 cells to saccharin (3 mM) 0 min (white bars) and 60 min (gray bars) subsequent to preincubation with gurmarin mutants (30 µg/mL). Control signal level is indicated by the dotted line (w/o gurmarin preincubation).

mutations into hydrophobic cluster positions led to a strong right-shift of the inhibition responses and severely increased the IC_{50} values to 4 and 7 µg/mL for gurmarin Y14A and L9A, respectively. Preincubation with the gurmarin mutant W28A was not sufficient to entirely block rT1r2/rT1r3-mediated fluorescence signals to saccharin within the range of the maximum applicable concentration of 30 µg/mL, thus precluding calculation of the IC_{50}. However, at the 2 highest test concentrations (10 and 30 µg/mL), the cellular signal of saccharin was significantly attenuated by pretreatment with gurmarin W28A (P = 0.0376 [df/F 0.0003–1 µg/mL vs. 10 µg/mL]; P = 0.0001 [df/F 0.0003–1 µg/mL vs. 30 µg/mL]). As expected, the gurmarin mutant W29A failed to exert any detectable suppressive effect on the rT1R2/rT1R3-mediated saccharin responses, indicating a loss or at least severe disruption of the protein functional integrity.

Furthermore, we conducted repeated calcium imaging measurements to keep track of the time cells required to recover from gurmarin treatment. During animal experiments, sweet taste inhibition by gurmarin was reversible but persistent (Imoto et al. 1991a; Murata et al. 2003). Whether this effect occurs at the receptor level or during signal transmission to the central nervous system has not yet been investigated. Fluorescence responses to saccharin (3 mM, according to Imoto et al. 1991a) of HEK293T Gα16gust44 cells expressing rT1r2/rT1r3 were entirely blocked directly after preincubation with wild-type gurmarin (30 µg/mL; Figure 6C, T = 0 min). Despite 3 interim washing procedures, the suppressive effect lasted to its full extend up to 1 h after removal of wild-type gurmarin (Figure 6C, T = 60 min). This observation suggests that the persistence of sweet taste suppression exerted by gurmarin occurs already at the level of the taste receptor cell and not during transmission or central processing of the taste signal. A decline in vitality of the cells precluded an extension of the measurements to more than 60 min. Thus, it remains to be determined, whether the time course in heterologous sweet taste receptor cells resembles the recovery after gurmarin treatment in vivo. By contrast, the in any case incomplete blocking of saccharin responses from cells preincubated with gurmarin hydrophobic cluster mutants L9A, Y14A, and W28A recovered completely within 60 min (Figure 6C). After 1 h, cells that had been treated with any of the gurmarin mutants elicited fluorescence signals upon saccharin application to a comparable extend as untreated cells (Figure 6C column 1 vs. 2–4). Thus, mutation of hydrophobic cluster residues L9, Y14, and W28 diminishes not only the potency of the protein inhibitor, but the persistence of the blocking effect as well.

Discussion

Gurmarin is an herbal sweet taste–inhibiting protein composed of 35 amino acid residues and 3 disulfide bridges that is known to specifically inhibit the rodent T1r2/T1r3 sweet taste receptor. Gurmarin is a member of the knottin family, a structural family of proteins that share little sequence homology apart from a common fold in which one disulfide bond threads though a macrocycle created by 2 other disulfide bonds and the peptide backbone (Arai et al. 1995; Fletcher et al. 1999). Here, we report the crystallographic structure of recombinant gurmarin secreted by the methylotrophic yeast *P. pastoris*. We found that the crystal structure contains a secondary structure and folds similar to those found in the solution structures of natural or synthetic gurmarin. Interestingly, the X-ray structure of gurmarin reveals highly mobile residues in 2 hydrophobic regions. The first region consists of 2 tryptophan residues (W28 and W29), and the second region consists of a larger hydrophobic patch that includes tyrosine residues Y13 and Y14. By combining site-directed mutagenesis and cellular functional assays, we found that alanine substitution of the amino acid residues located in these hydrophobic regions severely impaired the gurmarin inhibition properties towards the rT1R2/rT1R3 sweet taste receptor. These data suggest a direct interaction of gurmarin with the sweet taste receptor via these amino acid residues. We hypothesize that the high flexibility of these hydrophobic regions plays a role in the protein–protein (gurmarin-rT1r2/rT1r3) interaction. Although the exact mechanism of gurmarin inhibition is not known, we previously proposed 2 possible models in which the N-terminal domains of rT1r2/rT1r3 are bound to gurmarin (Sigoillot *et al.* 2012b). Unfortunately, the gurmarin mutagenesis data reported here does not allow to select a docking model. Site-directed mutagenesis of amino acid residues present in the sweet taste receptor would be necessary to confirm or infirm docking studies. Our results also emphasize that gurmarin may be a promising tool to decipher the molecular mechanism of the function of rodent T1r2/T1r3. Indeed, structures of inhibitors determined by use of X-ray techniques, when available, are generally suitable for use as molecular replacement templates and are a good starting point for the structural determination of protein complexes.

PDB deposition

The coordinates and diffraction data of gurmarin have been deposited into the PDB with accession code 5OLL.

Funding

This work was supported by a grant from Agence Nationale de la Recherche (ANR-09-ALIA-010). This work was also supported by INRA and Burgundy council (Région Bourgogne) grants to M.S.

Acknowledgments

The authors would like to thank Ms. Shila Fatehi for generating the PEAKrapid mGα15 stable cell line. Furthermore, we are indebted to Ms. Peggy Grossmann for her excellent technical assistance.

References

Arai K, Ishima R, Morikawa S, Miyasaka A, Imoto T, Yoshimura S, Aimoto S, Akasaka K. 1995. Three-dimensional structure of gurmarin, a sweet taste-suppressing polypeptide. *J Biomol NMR*. 5:297–305.

Ariyasu T, Matsumoto S, Kyono F, Hanaya T, Arai S, Ikeda M, Kurimoto M. 2003. Taste receptor T1R3 is an essential molecule for the cellular recognition of the disaccharide trehalose. *In Vitro Cell Dev Biol Anim*. 39:80–88.

Behrens M, Meyerhof W. 2011. Gustatory and extragustatory functions of mammalian taste receptors. *Physiol Behav*. 105:4–13.

Belloir C, Neiers F, Briand L. 2017. Sweeteners and sweetness enhancers. *Curr Opin Clin Nutr Metab Care*. 20:279–285.

Bricogne G, Blanc E, Brandl M, Flensburg C, Keller P, Paciorek W, Roversi P, Sharff A, Smart O, Vonrhein C. 2017. *BUSTER version 2.1.10*. Cambridge (England): Global Phasing Limited.

Chen VB, Arendall WB III, Headd JJ, Keedy DA, Immormino RM, Kapral GJ, Murray LW, Richardson JS, Richardson DC. 2010. MolProbity: all-atom structure validation for macromolecular crystallography. *Acta Crystallogr D Biol Crystallogr*. 66:12–21.

Emsley P, Lohkamp B, Scott WG, Cowtan K. 2010. Features and development of Coot. *Acta Crystallogr D Biol Crystallogr*. 66:486–501.

Fletcher JI, Dingley AJ, Smith R, Connor M, Christie MJ, King GF. 1999. High-resolution solution structure of gurmarin, a sweet-taste-suppressing plant polypeptide. *Eur J Biochem*. 264:525–533.

Gutmanas A, Alhroub Y, Battle GM, Berrisford JM, Bochet E, Conroy MJ, Dana JM, Fernandez Montecelo MA, van Ginkel G, Gore SP, *et al.* 2014. PDBe: Protein Data Bank in Europe. *Nucleic acids research* 42: D285–291.

Imoto T, Miyasaka A, Ishima R, Akasaka K. 1991a. A novel peptide isolated from the leaves of *Gymnema sylvestre*–I. Characterization and its suppressive effect on the neural responses to sweet taste stimuli in the rat. *Comp Biochem Physiol A Comp Physiol*. 100:309–314.

Imoto T, Miyasaka A, Ishima R, Akasaka K. 1991b. A novel peptide isolated from the leaves of *Gymnema sylvestre*–I. Characterization and its suppressive effect on the neural responses to sweet taste stimuli in the rat. *Comp Biochem Physiol A Comp Physiol*. 100:309–314.

Kabsch W. 2010. XDS. *Acta Crystallogr D Biol Crystallogr*. 66:125–132.

Kimura RH, Levin AM, Cochran FV, Cochran JR. 2009. Engineered cystine knot peptides that bind alphavbeta3, alphavbeta5, and alpha5beta1 integrins with low-nanomolar affinity. *Proteins*. 77:359–369.

Kniazeff J, Prézeau L, Rondard P, Pin JP, Goudet C. 2011. Dimers and beyond: The functional puzzles of class C GPCRs. *Pharmacol Ther*. 130:9–25.

Kohno D, Koike M, Ninomiya Y, Kojima I, Kitamura T, Yada T. 2016. Sweet taste receptor serves to activate glucose- and leptin-responsive neurons in the hypothalamic arcuate nucleus and participates in glucose responsiveness. *Front Neurosci*. 10:502.

Kojima I, Nakagawa Y, Ohtsu Y, Medina A, Nagasawa M. 2014. Sweet taste-sensing receptors expressed in pancreatic β-cells: sweet molecules act as biased agonists. *Endocrinol Metab (Seoul)*. 29:12–19.

Krissinel E. 2012. Enhanced fold recognition using efficient short fragment clustering. *J Mol Biochem*. 1:76–85.

Li X, Staszewski L, Xu H, Durick K, Zoller M, Adler E. 2002. Human receptors for sweet and umami taste. *Proc Natl Acad Sci USA*. 99: 4692–4696.

Maîtrepierre E, Sigoillot M, Le Pessot L, Briand L. 2012. Recombinant expression, in vitro refolding, and biophysical characterization of the N-terminal domain of T1R3 taste receptor. *Protein Expr Purif*. 83:75–83.

Margolskee RF, Dyer J, Kokrashvili Z, Salmon KS, Ilegems E, Daly K, Maillet EL, Ninomiya Y, Mosinger B, Shirazi-Beechey SP. 2007. T1R3 and gustducin in gut sense sugars to regulate expression of Na+-glucose cotransporter 1. *Proc Natl Acad Sci USA*. 104: 15075–15080.

Medina A, Nakagawa Y, Ma J, Li L, Hamano K, Akimoto T, Ninomiya Y, Kojima I. 2014. Expression of the glucose-sensing receptor T1R3 in pancreatic islet: changes in the expression levels in various nutritional and metabolic states. *Endocr J*. 61:797–805.

Miyasaka A, Imoto T. 1995. Electrophysiological characterization of the inhibitory effect of a novel peptide gurmarin on the sweet taste response in rats. *Brain Res*. 676:63–68.

Moore SJ, Hayden Gephart MG, Bergen JM, Su YS, Rayburn H, Scott MP, Cochran JR. 2013. Engineered knottin peptide enables noninvasive optical imaging of intracranial medulloblastoma. *Proc Natl Acad Sci USA* 110: 14598–14603.

Murata Y, Nakashima K, Yamada A, Shigemura N, Sasamoto K, Ninomiya Y. 2003. Gurmarin suppression of licking responses to sweetener-quinine mixtures in C57BL mice. *Chem Senses*. 28:237–243.

Nelson G, Hoon MA, Chandrashekar J, Zhang Y, Ryba NJ, Zuker CS. 2001. Mammalian sweet taste receptors. *Cell*. 106:381–390.

Nie Y, Vigues S, Hobbs JR, Conn GL, Munger SD. 2005. Distinct contributions of T1R2 and T1R3 taste receptor subunits to the detection of sweet stimuli. *Curr Biol*. 15:1948–1952.

Ninomiya Y, Imoto T. 1995. Gurmarin inhibition of sweet taste responses in mice. *Am J Physiol*. 268:R1019–R1025.

Ota M, Shimizu Y, Tonosaki K, Ariyoshi Y. 1998. Role of hydrophobic amino acids in gurmarin, a sweetness-suppressing polypeptide. *Biopolymers*. 45:231–238.

Pallaghy PK, Nielsen KJ, Craik DJ, Norton RS. 1994. A common structural motif incorporating a cystine knot and a triple-stranded beta-sheet in toxic and inhibitory polypeptides. *Protein Sci*. 3:1833–1839.

Pin JP, Galvez T, Prézeau L. 2003. Evolution, structure, and activation mechanism of family 3/C G-protein-coupled receptors. *Pharmacol Ther*. 98:325–354.

Postic G, Gracy J, Périn C, Chiche L, Gelly JC. 2018. KNOTTIN: the database of inhibitor cystine knot scaffold after 10 years, toward a systematic structure modeling. *Nucleic Acids Res*. 46:D454–D458.

Sheldrick GM. 2008. A short history of SHELX. ~~*Acta crystallographica. Section A, Foundations of crystallography* 64:112–122.~~

Sigoillot M, Brockhoff A, Lescop E, Poirier N, Meyerhof W, Briand L. 2012a. Optimization of the production of gurmarin, a sweet-taste-suppressing protein, secreted by the methylotrophic yeast *Pichia pastoris*. *Appl Microbiol Biotechnol*. 96:1253–1263.

Sigoillot M, Brockhoff A, Meyerhof W, Briand L. 2012b. Sweet-taste-suppressing compounds: current knowledge and perspectives of application. *Appl Microbiol Biotechnol*. 96:619–630.

Sreerama N, Manning MC, Powers ME, Zhang JX, Goldenberg DP, Woody RW. 1999. Tyrosine, phenylalanine, and disulfide contributions to the circular dichroism of proteins: circular dichroism spectra of wild-type and mutant bovine pancreatic trypsin inhibitor. *Biochemistry*. 38:10814–10822.

Vancleef L, Van Den Broeck T, Thijs T, Steensels S, Briand L, Tack J, Depoortere I. 2015. Chemosensory signalling pathways involved in sensing of amino acids by the ghrelin cell. *Sci Rep*. 5:15725.

AQ10